SLAC-PUB-9133

March 2002

(A)

A Very High Charge, High Polarization Gradient-Doped Strained GaAs Photocathode*

T. Maruyama, A. Brachmann, J. E. Clendenin, T. Desikan,

E. L. Garwin, R. E. Kirby, D.-A. Luh, and J. Turner

Stanford Linear Accelerator Center, Stanford, California 94309

R. Prepost

Department of Physics, University of Wisconsin, Madison, Wisconsin 53706

Submitted to Nuclear Instruments and Method A

*This work was supported by Department of Energy contract DE–AC03–76SF00515(SLAC) and DE-FG02-95ER40896(Wisconsin).

A Very High Charge, High Polarization Gradient-Doped Strained GaAs Photocathode

T. Maruyama,* A. Brachmann, J. E. Clendenin, T. Desikan

E. L. Garwin, R. E. Kirby, D.-A. Luh, and J. Turner

Stanford Linear Accelerator Center, Stanford, California 94309

R. Prepost

Department of Physics, University of Wisconsin, Madison, Wisconsin 53706

Abstract

A high-gradient-doping technique is applied to strained polarized photocathodes. The electron spin-polarization increases significantly as the highly-doped layer thickness is reduced. A 5.0 - 7.5 nm p-type surface layer doped to 5×10^{19} cm^{-3} is found sufficient to overcome the surface charge limit. It is shown that the charge requirements of the Next Linear Collider can be met with a polarization approaching 80%.

PACS: 29.25.Bx; 73.50.Pz; 73.61.Ey; 79.60.-i

Keywords: Polarized electron source; GaAs photocathode

---

*Corresponding author. Tel.: 650-926-3398; fax: 650-926-3718. *E-mail address:* tvm@slac.stanford.edu (T. Maruyama)

I. INTRODUCTION.

Polarized electron sources based on photoemission from negative-electron-affinity (NEA) III-V semiconductor photocathodes have been widely used for linear electron accelerators. Since 1992 the SLAC 3-km linac has used polarized electrons exclusively, not only for the Stanford Linear Collider (SLC) and fixed-target experiments that require polarization, but also when polarization is not required, such as for filling the PEP II storage rings. Strained, medium-doped (5×10^{18} cm^{-3}), GaAs photocathodes were introduced for the polarized electron source [1] in 1993. These photocathodes are capable of producing up to 1×10^{11} electrons in a 2 ns pulse with 75-85% polarization. However, they are susceptible to the surface charge limit (SCL): the total photoemitted charge in a short bunch saturates as the light intensity is increased. The SCL phenomenon was first observed using bulk GaAs [2], and several experimental studies have been made on strained GaAs [3], superlattice structures [4], and thin unstrained GaAs [5]. In reference [6] the SCL was attributed to a photovoltage effect in the band bending region, which momentarily increases the surface work function and thus suppresses emission.

The SCL poses a serious problem for operation of polarized electron sources at future linear colliders such as the Japan Linear Collider (JLC) and the Next Linear Collider (NLC) [7]. The NLC is presently designed to operate with a train of 190 micro-bunches, spaced 1.4 ns apart, and each micro-bunch is required to have as much as 1.4×10^{10} e$^-$ per pulse in 0.5 ns (full width) at the gun (4.4 A assuming a Gaussian charge distribution), totaling 2.7×10^{12} e$^-$ per train. The standard SLAC strained photocathodes saturate at a level of 8×10^{11} e$^-$ for a 300-ns pulse (0.4 A), well below the space charge limit of the gun. A recent study showed that the SCL problem can be reduced significantly by increasing the p-type doping concentration to at least 2×10^{19} cm^{-3} [8]. However, increasing the doping level leads to some depolarization of the electron spin. To increase the doping level without spin depolarization, a high-gradient-doping technique has been explored. While a standard SLAC photocathode is uniformly doped at 5×10^{18} cm^{-3}, we have reduced the active layer

dopant density to 5×10^{17} cm^{-3} while increasing the density of a 10-nm surface layer to 5×10^{19} cm^{-3}. The lower-than-standard doping level in the active layer avoids depolarization, while the high surface doping addresses the charge limit problem. A high-gradient-doping technique was applied first to a superlattice structure as a way to increase polarization [9], and more recently to address the SCL with a superlattice structure [4]. In the present paper we describe the first application of the high-gradient-doping technique to a strained-layer structure, and demonstrate for the first time that an NLC compatible charge with polarization approaching 80% is achievable.

II. PHOTOCATHODES

The samples for the present experiment were grown by Bandwidth Semiconductor, LLC. [10] using metal-organic-chemical-vapor-deposition (MOCVD). Figure 1 shows the photocathode structure. A 0.25 μm-thick p-type GaAs buffer layer was grown on a (100) p-type GaAs substrate oriented 2° towards the (110) direction. In order to produce a strain-relieved $GaAs_{1-x}P_x$ layer on GaAs, a 2.5 μm-thick $GaAs_{1-x'}P_{x'}$ layer was grown with a linearly increasing phosphorus fraction from 0 to x to accommodate the lattice mismatch, followed by an additional 2.5 μm-thick $GaAs_{1-x}P_x$ layer with a fixed phosphorus fraction. The lattice-mismatched active photoemission layer was then grown on this layer. The active layer with thickness from 55 to 90 nm was GaAs or $GaAs_{0.95}P_{0.05}$. The lattice-mismatch between the active layer and the $GaAs_{1-x}P_x$ layer was 1%. The active layers were p-type doped with zinc to a value of 5×10^{17} cm^{-3}. On top of the active layer, the GaAs surface layer with thickness from 10 to 45 nm was grown with a doping concentration of 5×10^{19} cm^{-3}. In order to preserve an atomically clean surface the samples were anodized to form an oxide layer on the GaAs surface [11]. The oxide layer was later removed as described below. Table 1 summarizes the photocathodes used in the present experiment.

III. EXPERIMENTAL FACILITIES

A. Cathode Test System

Polarization and quantum efficiency (QE) [12] were first studied in the SLAC Cathode Test System (CTS) shown schematically in Figure 2. The CTS is an ultra-high vacuum system pumped by a combination of ion and non-evaporable getter (NEG) pumps. The system is equipped with a load-lock chamber through which samples can be introduced without venting the system vacuum. Polarization measurements are accomplished by an electron transport column, an electrostatic 90° spin-rotator and a 20 keV Mott polarimeter. The photon helicity is controlled by a linear-polarizer/liquid-crystal retarder combination.

Prior to installation in the system, the sample is degreased in a boiling solution of trichloroethane. After the protective oxide layer is removed in ammonium hydroxide, the sample is rinsed in distilled water and methanol. The cathode activation method used to obtain an NEA surface consists of heat cleaning to 600° C for 1 hour, cool-down for an hour, followed by application of cesium until the photo-yield peaks, and then cesium and nitrogen-trifluoride co-deposition until the photo-yield is again maximized. The heat-cleaning temperature is monitored via an infrared pyrometer. The cathode is activated while monitoring the photo-yield with a white light and a 670 nm diode laser. Once a red response is observed from the diode laser, the white light is turned off and the diode laser is used to complete the activation. The absolute QE is measured using the diode laser at a photon wavelength of 670 nm. A tungsten lamp and a monochrometer are used to measure the relative QE as a function of photon wavelength, and these measurements are then normalized to the diode laser measurement at 670 nm.

B. SLAC Gun Test Laboratory

The SLAC Gun Test Laboratory (GTL) is used to study the production of intense, highly-polarized electron beams required for the NLC. The laboratory, shown schemati-

cally in Figure 3, is a replica of the first few meters of the SLAC injector beamline. The GTL beamline consists of an ultra-high-vacuum, high-voltage electrostatic gun, a load-lock chamber for cathode transfer and activation (not shown in Figure 3), and a beamline with magnetic components for electron beam transport and steering. An electrically isolated, optically coupled nanoammeter is used to measure the average photoemission current. The cathode is biased at -120 kV and maintained at a temperature of $0 \pm 2^{\circ}$ C by circulating cold nitrogen gas. With the cathode biased at -120 kV, the field gradient at the cathode is 1.8 MV/m, and the gun is capable of extracting a space-charge-limited current of 15 A from the 20 mm diameter cathode. A fast Faraday cup is used to measure the temporal profile of the beam with a time resolution of 0.5 ns. The Faraday cup has a 2 mm diameter hole through which a fraction of the beam is transported to the Mott chamber for polarization measurements. The vacuum in the gun is maintained at about $1\text{x}10^{-11}$ Torr by means of ion and nonevaporative getter pumping. A more detailed description of the gun and load-lock system can be found in reference [1].

The cathode is activated in the GTL load-lock chamber. The cathode preparation and activation procedures are similar to those used for the CTS. The heat-cleaning temperature is measured at the back surface of the cathode holder using a thermocouple. The temperature at the cathode surface is estimated to be about 600° C when the thermocouple temperature is 800° C. Cathodes are typically heat-cleaned and activated twice before being moved into the gun. Once the cathode is moved into the gun, the cathode QE can be restored by application of cesium without further heat-cleaning or exposure to nitrogen trifluoride. The cathode lifetime is continuously monitored using a 750 nm diode laser running at 1.5 Hz and a lock-in amplifier to detect the modulated current of the nanoammeter.

C. Laser Systems

The NLC multi-bunch structure electron beam will be produced with a laser system having the same multi-bunch structure. The laser is required to have 3.5 μJ in each 0.5 ns

micro-bunch totaling 665 μJ for 190 bunches. Since such a laser system is not available, two presently available laser systems are used to simulate the NLC beam conditions.

Figure 4 shows the laser system used for the present experiment. A flashlamp-pumped Ti:Sapphire laser (Flash-Ti) operated at 60 Hz produces a 10 μs long pulse as shown in Figure 5. To produce a pulse equivalent to one NLC train, a 300-ns long pulse is sliced out of the 10 μs pulse using a crossed-polarizer pair and a Pockels cell (Slicer P.C.). When a pulse is sliced at t $\sim$ 7.5 μs (**Slice 1** in Figure 5), the pulse has a flat top shape, but the maximum energy is limited to 100 μJ/pulse. To increase the energy, a pulse is also sliced at t $\sim$ 1.5 μs (**Slice 2** in Figure 5). The maximum laser energy increases to 300 μJ/pulse, but the temporal shape is no longer flat. An additional polarizer and a Pockels cell (Intensity P.C.) are used to control the laser intensity. The wavelength of the laser is set by a retardation plate at the Brewster angle.

The second laser system (YAG-Ti) employs a commercial frequency-doubled Nd:YAG laser operated at 60 Hz to pump a Ti:sapphire cavity to produce a 4-ns long pulse. The Ti:sapphire cavity is Q-switched and cavity-dumped by an intracavity Pockels cell. The slicer that produces a 2-ns pulse and the intensity controller are bypassed for this experiment. The laser energy is about 20 μJ/pulse.

The lasers are circularly polarized through a quarter-wave retardation generated by a Pockels cell (Helicity P.C.). For both lasers, the energy is measured using a joule meter, the spot size on the cathode is varied by a telescope, and the beam spatial profile is analyzed by a CCD camera. Figure 6 shows the measured beam profile of the multi-mode Flash:Ti laser.

IV. HIGH-GRADIENT-DOPED GaAs

A. Sample Preparation

Since a high overall doping concentration would depolarize electron spin, the thickness of the highly-doped layer must be minimized. To study empirically how the polarization is affected by the highly-doped layer, the spin-polarization was measured for samples with different highly-doped layer thicknesses. The samples obtained from the vendor were grown on 50 mm diameter GaAs wafers with GaAs surface layers of different thickness as shown in Table I. An anodization/stripping technique was then used to prepare samples of different surface layer thickness for polarization and QE measurements. The anodization/stripping technique consisted of a self-terminating anodization at a given voltage forming an oxide layer [11] and a stripping of the resulting oxide layer in an ammonium hydroxide solution followed by rinsing in distilled water and methanol. Using this technique, the GaAs surface layer can be removed at the rate of 1.5 nm/V as described in the next section. For example, a sample from wafer #4505 was sequentially anodized at 5 V, 8.4 V, 1.9 V and 1.9 V, resulting in nominal surface layer thickness of 19.6 nm, 7.1 nm, 4.3 nm, and 1.4 nm based on an original surface layer thickness of 27 nm. A sample from wafer #4506, with an original surface layer thickness of 45 nm, was anodized once at 5 V resulting in a nominal surface layer thickness of 37.5 nm.

B. Secondary Ion Mass Spectroscopy

The doping concentration was designed to be 5×10^{17} cm^{-3} in the active layer and 5×10^{19} cm^{-3} in the surface layer. However, in actual wafers the concentration does not increase abruptly from 5×10^{17} cm^{-3} to 5×10^{19} cm^{-3}. It is necessary to measure the actual dopant profile and then calibrate the anodization rate using the measured profile. Furthermore, the dopant diffusion during the heat-cleaning is a concern as a rapid diffusion would destroy the high-gradient-doping profile. The GaAs evaporation during the 600° C heat-cleaning

must be considered as well. The depth profile of the dopant concentration was measured by Secondary Ion Mass Spectroscopy (SIMS), which is made by sputtering a sample surface with a primary ion beam (typically cesium or argon ions) followed by mass spectrometry of the emitted secondary ions [13].

SIMS analyses were performed on three samples from wafer #4505: 1) an unused sample; 2) a sample heat-cleaned for 4.75 hours at 600° C; and 3) a sample anodized at 5 V and stripped. Figure 7 shows the depth profile of the zinc concentration for these three samples. Comparing Samples 1 and 3, the anodization rate was determined to be 1.5 nm/V. Comparing Samples 1 and 2, the GaAs evaporation rate was $\approx$ 0.4 nm per 1 hour heat-cleaning at 600° C. The evaporation rate was significantly lower than the previously determined values [14]. This difference could be explained by the fact that the 12-mm-diameter cathode was not large enough to fill the field of view of the pyrometer. Consequently the pyrometer picked up radiation from the sample holder, which is typically at 800° C during heat-cleaning. The actual surface temperature was estimated to be about 560° C. The zinc diffusion seemed negligible as the zinc concentration profiles were the same between Samples 1 and 2. However, there was some indication of zinc diffusing out of the surface.

C. Polarization and Charge Measurements

The polarization and QE measurements were performed in the CTS. Each measurement consisted of anodization/stripping, introduction to the vacuum system through a load-lock, 1 hour heat-cleaning at 600° C, 1 hour cool-down, an activation with cesium and nitrogen-trifluoride using co-deposition, then a QE measurement followed by polarization measurements. Figure 8 shows the polarization and QE as a function of wavelength for a sample from wafer #4505 with nominal surface surface layer thickness of (a) 19.6 nm, (b) 7.1 nm, (c) 4.3 nm and (d) 1.4 nm. Figure 9 shows the peak polarization as a function of the highly-doped layer thickness. The polarization increased significantly as the highly-doped layer thickness was reduced, reaching 80% polarization with about 7.5 nm of the highly-doped layer.

The CTS study has thus shown that it is possible to reach 80% polarization with about 7.5 nm of a highly-doped layer. The next question is whether 7.5 nm of highly-doped layer is thick enough to overcome the SCL problem. The GTL was used to study the charge performance. A sample from wafer #4505 was anodized at 13 V so that the thickness of the remaining high-doped layer was 7.5 nm. The sample was then heat-cleaned and activated twice in the load-lock system. The polarization was measured as a function of the Flash-Ti laser wavelength from 820 nm to 850 nm, yielding a peak polarization of 77% at 835 nm, consistent with the data shown in Figure 9. The QE at 835 nm was 0.09%, which was about a factor of two lower than the QEs expected for strained photocathodes. The charge measurements were performed using the laser wavelength of 835 nm. Figure 10 shows the temporal profiles of the emission current pulses measured using varying Flash-Ti laser energies. The laser pulse was sliced at **Slice 1** in Figure 5. As the laser energy was increased, the temporal profile simply scaled without developing the leading edge spike typically observed in the surface-charge-limited photoemission [8]. Figure 11 shows the charge output as a function of the Flash-Ti laser energy. The observed charge output increases linearly with the laser energy, reaching 8×10^{11} e^-/pulse. Although the sample did not show any charge limit behavior, the QE was lower than expected. The low QE was thought to be due to the energy barrier in the conduction band [15].

V. HIGH-GRADIENT-DOPED STRAINED GaAsP

A. Charge measurements at the GTL

To remove the energy barrier in the conduction band, the active layer was changed to $GaAs_{0.95}P_{0.05}$. The 5% phosphorus raised the conduction band by 58 meV compensating the energy difference due to the high gradient doping. Figure 12 shows schematically the conduction bands expected for the two structures. The QE and polarization of a photocathode from wafer #5868 measured at low voltage in the CTS are shown in Figure 13. A QE of

0.2% and peak polarization of 80% were measured at room temperature. The wavelength at the peak polarization was about 805 nm. The 40-nm blue shift with respect to a standard strained GaAs cathode is due to the larger band gap energy of the $GaAs_{0.95}P_{0.05}$ active layer. The higher QE can be attributed to the absence of a surface energy barrier resulting from the larger band gap energy.

A sample from wafer #5868 was heat-cleaned and activated twice in the load-lock system, and the charge measurements were made over a six week period. Figure 14 shows a typical QE variation over ten days. The QE decreased by approximately 10% (δQE/QE) per day, and the cathode was cesiated every third day. The QE (at 780 nm) after cesiation was typically 0.4%. Figure 15 shows the charge output as a function of the Flash-Ti laser energy. The two data sets were taken for the cathode before cesiation when the QE was the lowest (0.3%) and after cesiation when the QE was the highest (0.4%). For both cases the charge output was proportional to the laser energy, and no charge saturation was observed.

Since the charge output was limited by the laser energy, the slice timing was changed to **Slice 2** in Figure 5, and the photon density was increased by reducing the laser spot size. However, as the laser spot size was reduced, the photoemission was limited by the space charge limit effect of the gun. Figures 16 a) and 16 b) show the charge output as a function of the laser spot size for the Flash-Ti and YAG-Ti, respectively. With a spot size larger than about 10 mm for Flash-Ti and about 14 mm for YAG-Ti, the charge output was limited by the laser energy. As the laser spot size was reduced, the charge output decreased due to the space charge limit. The best operating diameter for achieving the highest photon density was about 14 mm where the photoemission was not affected by the space charge limit. The laser spot size of both lasers was set to 14 mm, and the Flash-Ti pulse length was set to 270 ns. The charge output was measured as a function of the Flash-Ti laser energy. The YAG-Ti laser was then overlaid on the Flash-Ti laser. While the YAG-Ti laser energy was fixed at 20 μJ/pulse, the charge output was measured as the Flash-Ti laser energy was increased. Figure 17 shows the charge output as a function of the Flash-Ti laser energy with and without the YAG-Ti laser. The YAG-Ti laser by itself produced 2.3×10^{11} e^-/pulse,

equivalent to 9.2 A peak current (assuming a Gaussian pulse), twice the NLC requirement. The charge output was again linear up to the maximum laser energy, producing a maximum charge of 2.2×10^{12} e^- in 270 ns. If one assumes a linear scaling with spot size, this charge is equivalent to 4.5×10^{12} e^- (2.6 A) from a 20 mm diameter cathode.

B. Performance at the accelerator

A SLAC high energy experiment, E158, to measure parity violation in Möller scattering ($e^-e^- \rightarrow e^-e^-$) will use a 48 GeV polarized electron beam scattering off unpolarized electrons in a liquid hydrogen target [16]. The experiment requires a beam intensity of 8×10^{11} e^- in a 370 ns pulse at the gun. Since the beam intensity requirement is difficult to meet using the standard SLAC photocathodes, it was proposed to use the newly developed high-gradient-doped GaAsP photocathode described herein. A sample from wafer #5868 was installed in the SLAC polarized electron source and heat-cleaned and activated twice. The initial QE was 0.4% at 805 nm. The excitation light source was a flashlamp-pumped Ti:Sapphire laser, identical to the Flash-Ti laser described in Section III.A, and the 20 mm diameter photocathode was fully illuminated. Figure 18 shows the charge output as a function of the laser energy for a 100-ns long pulse. The charge output was linear up to the maximum laser energy, producing a maximum charge of 2.3×10^{12} e^- in 100 ns (3.7 A), which is nearly equal to the peak current required for the NLC. Finally the charge output was observed to scale with the laser pulse length, reaching more than 8×10^{12} e^- for 370 ns. The charge output corresponds to ten times the E158 requirement and more than twice the NLC-train charge. The QE was allowed to decrease and the diameter of the illuminated area was reduced to 14 mm diameter. The charge output was still linear up to the maximum laser energy as shown in Figure 18. Again assuming a linear scaling with spot size, a peak current that exceeds the NLC requirement can be expected from a 20 mm diameter cathode.

VI. CONCLUSIONS

The charge capabilities of high-gradient-doped strained photocathodes have been determined. A charge as large as 2.2×10^{12} e^- per pulse was produced from a 14-mm diameter laser spot in 270 ns. By overlaying a short pulse laser, the peak current capability was also determined. A peak current as high as 9.2 A was extracted. There were no indications of a surface charge limit even when the QE decreased, and the charge output was limited by the laser energy. A cathode of this type is being used in a current high energy polarization experiment at SLAC, for which the charge performance has been consistent with, if not superior to, the laboratory results. This is the first demonstration that a NLC compatible beam with polarization approaching 80% is achievable.

Acknowledgments

We thank G. Mulhollan for his contribution to the early part of this work, and T. Galetto for technical assistance. This work was supported by Department of Energy contract DE–AC03–76SF00515(SLAC) and DE-FG02-95ER40896(Wisconsin).

REFERENCES

[1] R. Alley, et al., Nucl. Instrum. Meth. A 365 (1995) 1.

[2] M. Woods, et al., J. Appl. Phys. 73 (1993) 8531.

[3] H. Tang, *Proceedings of the Workshop on Photocathodes for Polarized Electron Sources for Accelerators*, SLAC-PUB 432 Rev (1993) 344.

[4] Y. Kurihara et al., Jpn. J. Appl. Phys. 34 (1995) 355; K. Togawa et al., Nucl. Instrum. Meth. A 414 (1998) 431; K. Togawa et al., Nucl. Instrum. Meth. A455, (2000) 118.

[5] A.S.Jaroshevich et al., 7-th International Workshop on Polarized Gas Targets and Polarized beams, Urbana, USA, 1997, edited by R.J. Holt and M.A. Miller. AIP Conference Proceedings, 421 (1998) 549.

[6] A. Herrera-Gómez, G Vergara and W. E. Spicer, J. Appl. Phys. 79 (1996) 7318.

[7] *JLC Design Study*, KEK-Report 97-01 (1997); *Zeroth Order Design Report for the Next linear Collider*, SLAC Report 474, May 1996. Another proposed collider TESLA (*TESLA Technical Design Report*, DESY-2001-011, March 2001), however, dos not have the charge limit problem as the time separation between bunches is 300 ns.

[8] G.A. Mulhollan, A.V. Subashiev, J.E. Clendenin, E.L. Garwin, R.E. Kirby, T. Maruyama , and R. Prepost, Phys. Lett. A282, (2001) 309.

[9] Y. Kurihara et al., Nucl. Instrum. Meth. A313 (1992) 393; T. Omori et at., Int. J. Mod. Phys. A (Proc. Suppl.) 2A (1993) 157.

[10] Bandwidth Semiconductor (former Spire Coorporation), Hudson, NH 03051 USA.

[11] B. Schwartz, F. Ermanis, and M. H. Brastad, J. Electrochem. Soc. 123 (1976) 1089.

[12] The quantum efficiency is measured as a number of photoemitted electrons per incident photon without correcting for the GaAs surface reflection and the window reflection.

[13] SIMS analyses were performed at Charles Evans & Associates, Sunnyvale, CA 94086 USA.

[14] J.S. Blakemore, J. Appl. Phys. 53 (1982) R123; R. Kirby, SLAC PolSource Tech Note 93-7 (1993) (unpublished); K. Burrows and G. Mulhollan, SLAC PolSource Tech Note 99-6 (1999) (unpublished).

[15] H.C. Casey and M.B. Panish, *Heterostructure Lasers*, Ch. 4, Academic Press, New York (1978).

[16] SLAC-PROPOSAL-E-158, July 1997.

TABLES

	wafer 4505	wafer 4506	wafer 5868
GaAs Surface Layer Thickness (nm)	27*	45	10
GaAs Surface Layer Doping (10^{19} cm^{-3})	5	5	5
Active Layer	GaAs	GaAs	$GaAs_{0.95}P_{0.05}$
Active Layer Thickness (nm)	75	55	90
Active Layer Doping (10^{17} cm^{-3})	5	5	5
Buffer Layer	$GaAs_{0.71}P_{0.29}$	$GaAs_{0.71}P_{0.29}$	$GaAs_{0.66}P_{0.34}$

TABLE I. Sample parameters. * The layer thickness was measured by SIMS.

LIST OF FIGURES

Figure 15 The photoemission charge per pulse as a function of the laser energy before and after cesiation for a sample from wafer #5868 measured at the GTL.

Figure 16 The photoemission charge per pulse as a function of the laser beam diameter for a fixed laser energy for a) long pulse Flash-Ti laser and b) short pulse YAG-Ti laser.

Figure 17 The photoemission charge per pulse as a function of the laser energy for Flash-Ti only (open circles) and Flash-Ti and YAG-Ti overlaid (solid circles) measured at the GTL.

Figure 18 The photoemission charge per pulse as a function of the laser energy for 0.31% QE and 20 mm diameter spot (solid circles) and 0.25% QE and 14 mm diameter spot (open circles) measured at the SLAC injector.

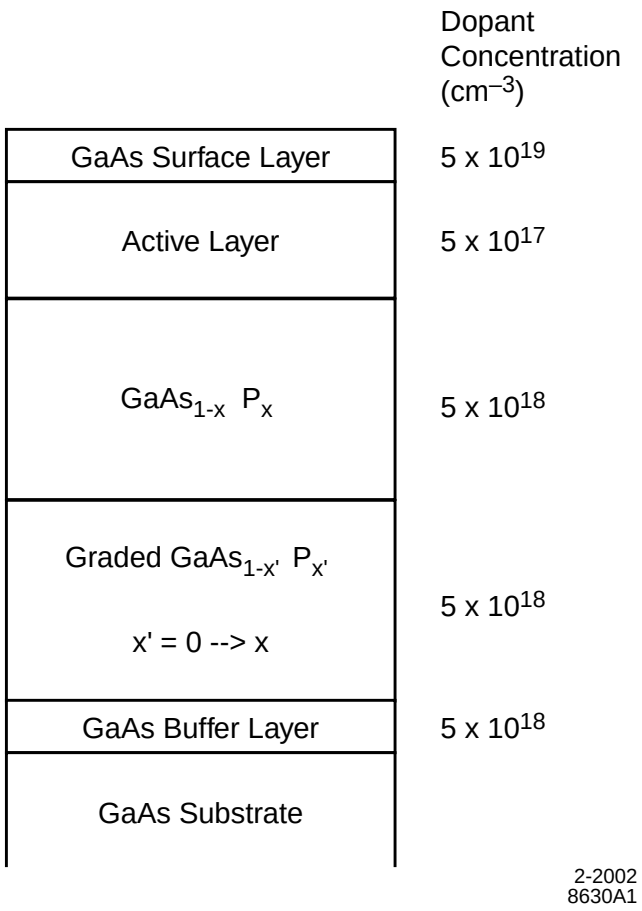
Dopant Concentration (cm^{-3})
GaAs Surface Layer
5×10^{19}
Active Layer
5×10^{17}
$GaAs_{1-x} P_x$
5×10^{18}
Graded $GaAs_{1-x'} P_{x'}$
x' = 0 --> x
5×10^{18}
GaAs Buffer Layer
5×10^{18}
GaAs Substrate
2-2002
8630A1

FIGURE 1

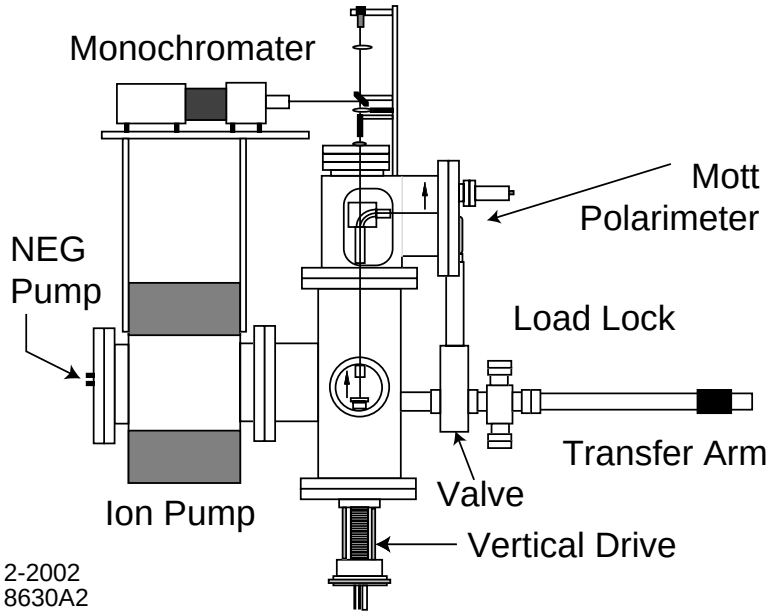
Monochromater
Mott
Polarimeter
NEG
Pump
Load Lock
Transfer Arm
Valve
Ion Pump
Vertical Drive
2-2002
8630A2

FIGURE 2

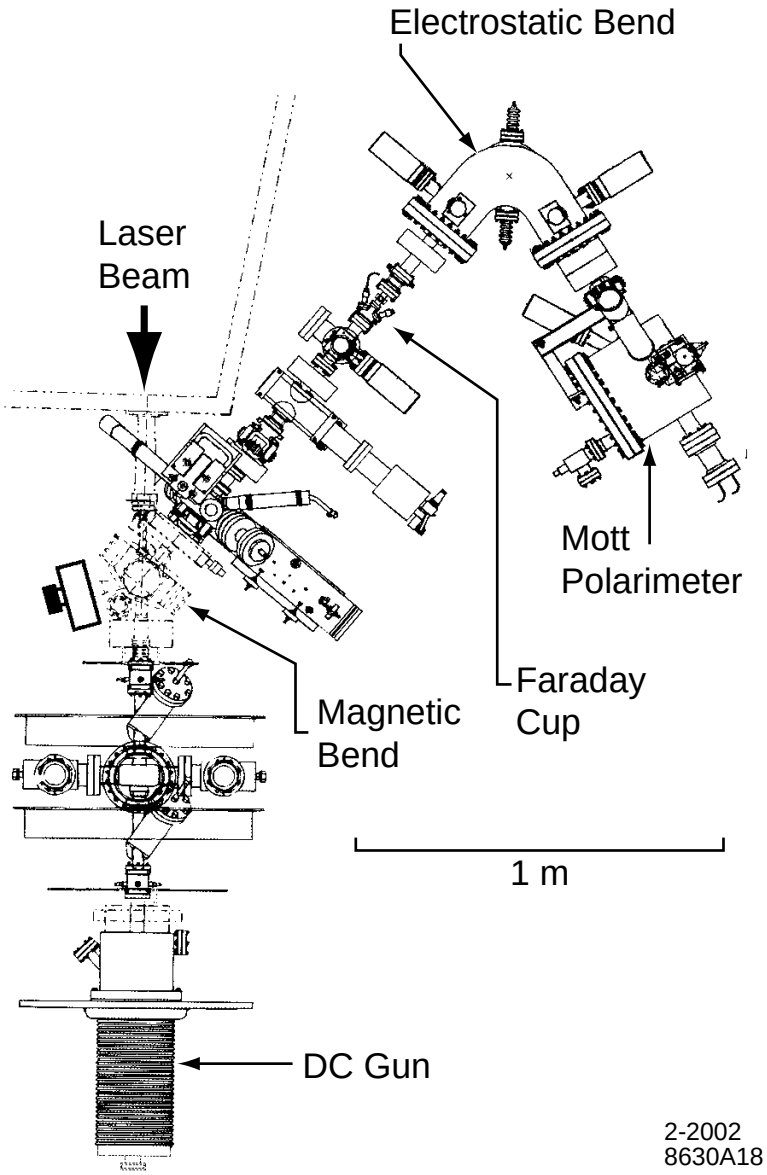
Electrostatic Bend
Laser
Beam
Mott
Polarimeter
Faraday
Cup
Magnetic
Bend
1 m
DC Gun
2-2002
8630A18

FIGURE 3

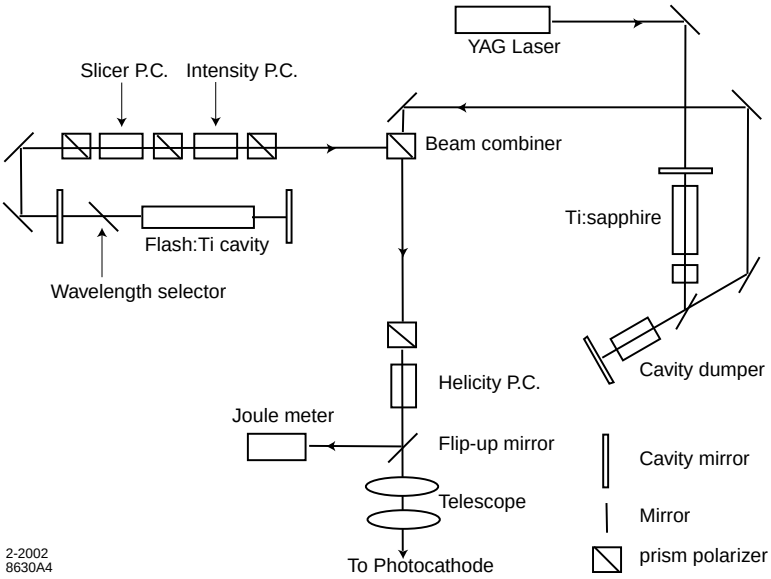
YAG Laser
Slicer P.C.
Intensity P.C.
Beam combiner
Ti:sapphire
Flash:Ti cavity
Wavelength selector
Cavity dumper
Helicity P.C.
Joule meter
Flip-up mirror
Cavity mirror
Telescope
Mirror
prism polarizer
To Photocathode
2-2002
8630A4

FIGURE 4

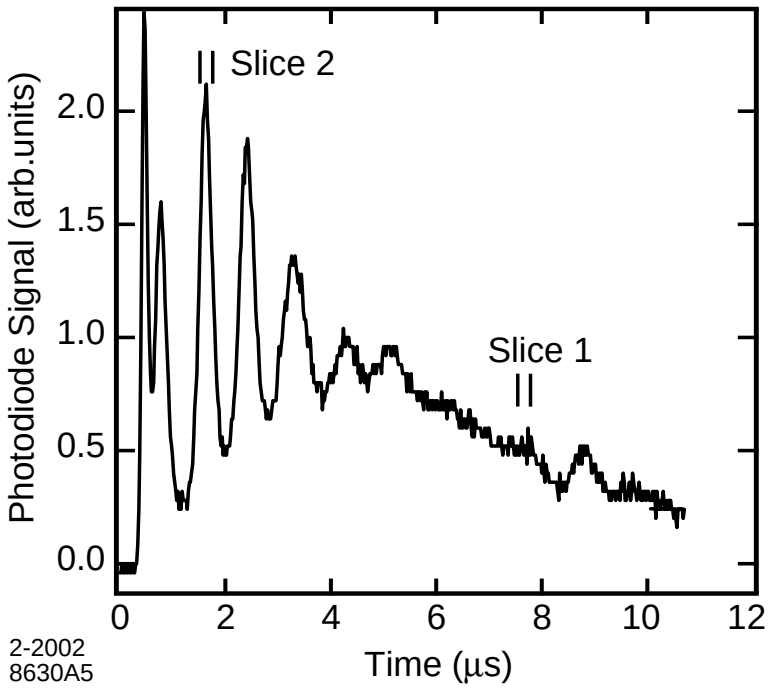
Slice 2
Slice 1
Photodiode Signal (arb.units)
2.0
1.5
1.0
0.5
0.0
0
2
4
6
8
10
12
Time (μs)
2-2002
8630A5

FIGURE 5

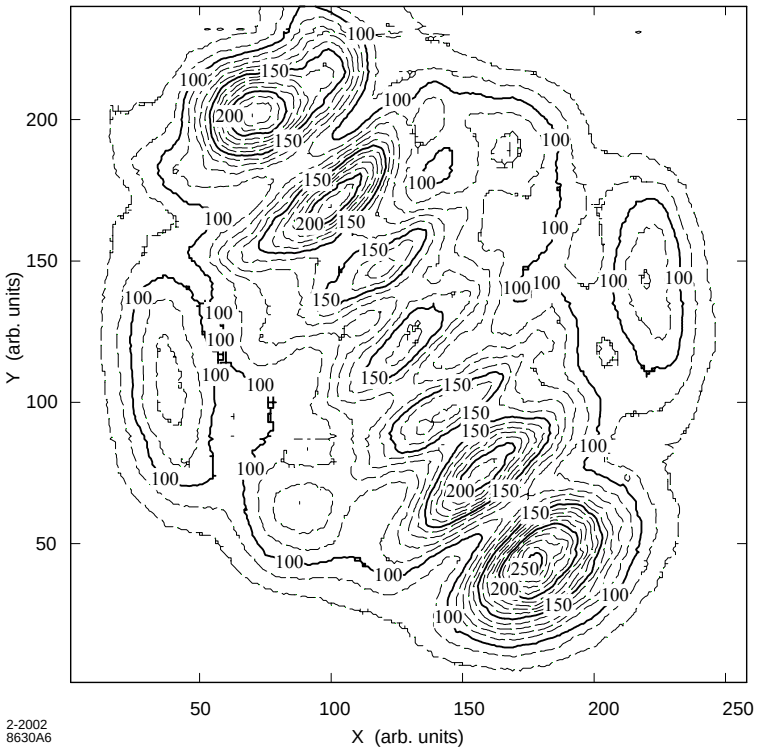

FIGURE 6

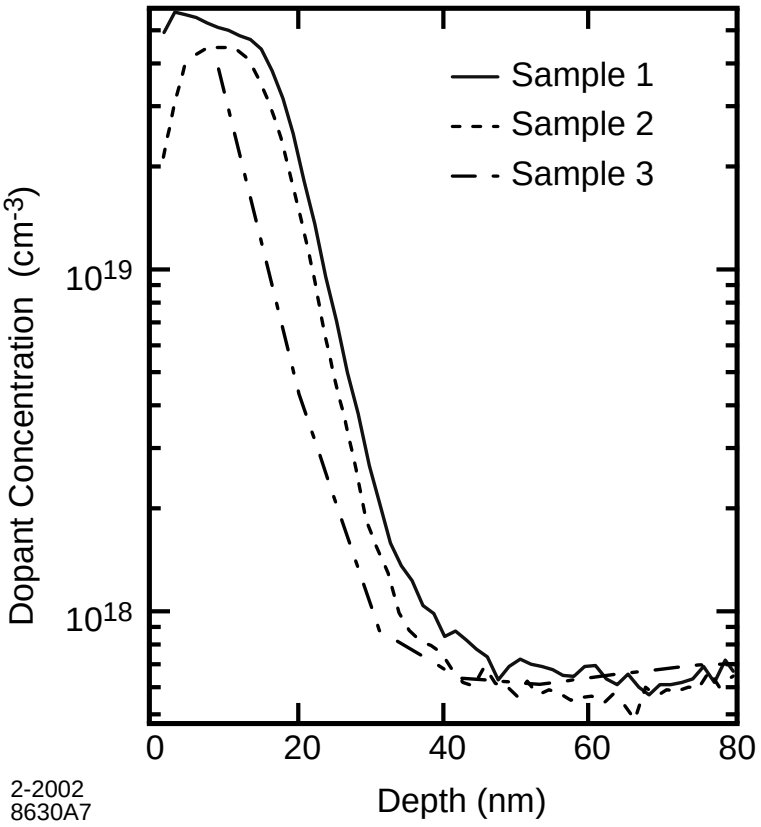
Sample 1
Sample 2
Sample 3
Dopant Concentration (cm-3)
10^19
10^18
0
20
40
60
80
Depth (nm)
2-2002
8630A7

FIGURE 7

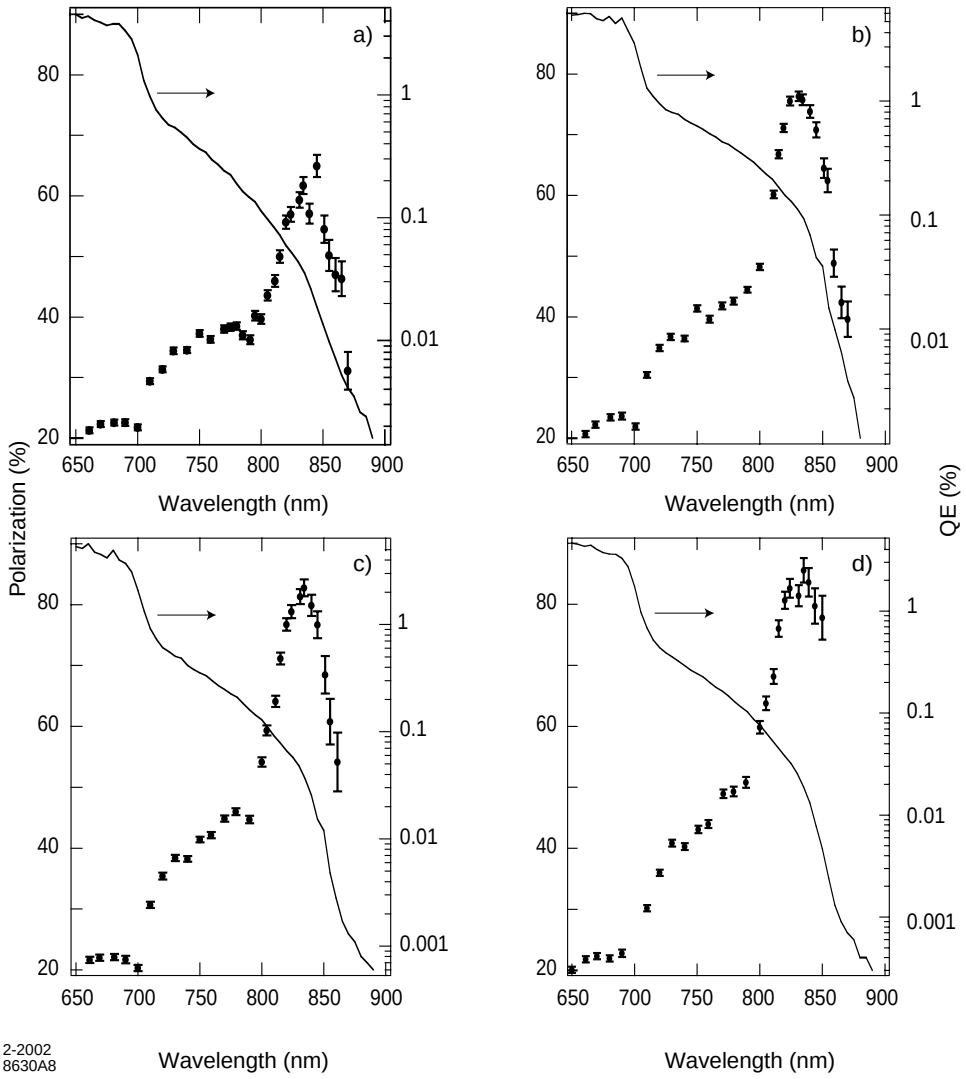
a)
b)
c)
d)
Polarization (%)
QE (%)
Wavelength (nm)
Wavelength (nm)
Wavelength (nm)
Wavelength (nm)
2-2002
8630A8

FIGURE 8

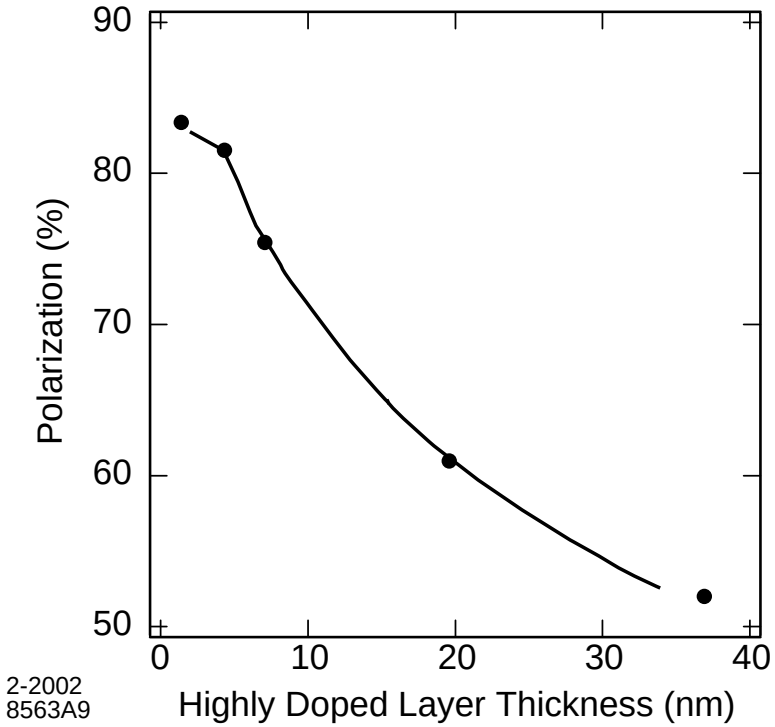
90
80
70
60
50
Polarization (%)
0
10
20
30
40
Highly Doped Layer Thickness (nm)
2-2002
8563A9

FIGURE 9

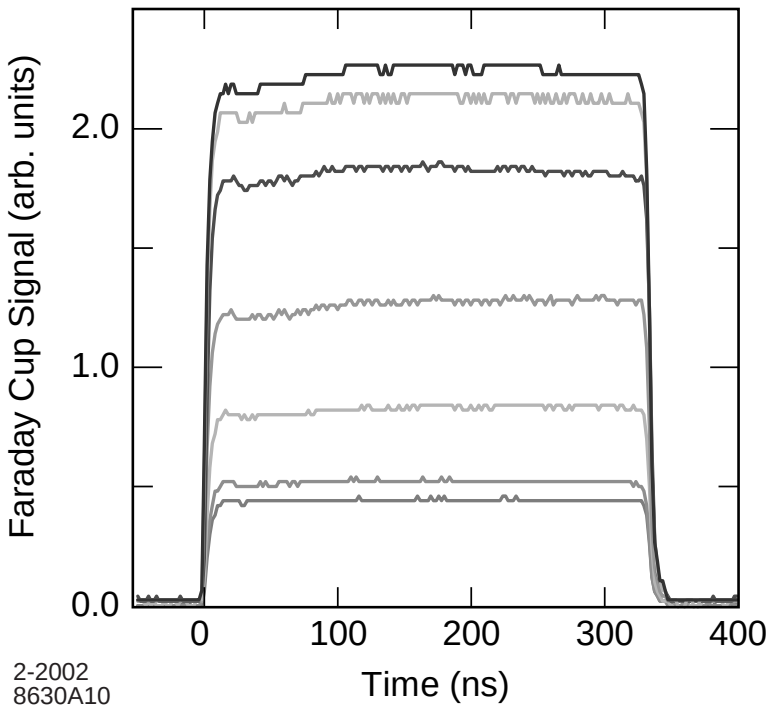
Faraday Cup Signal (arb. units)
2.0
1.0
0.0
0
100
200
300
400
Time (ns)
2-2002
8630A10

FIGURE 10

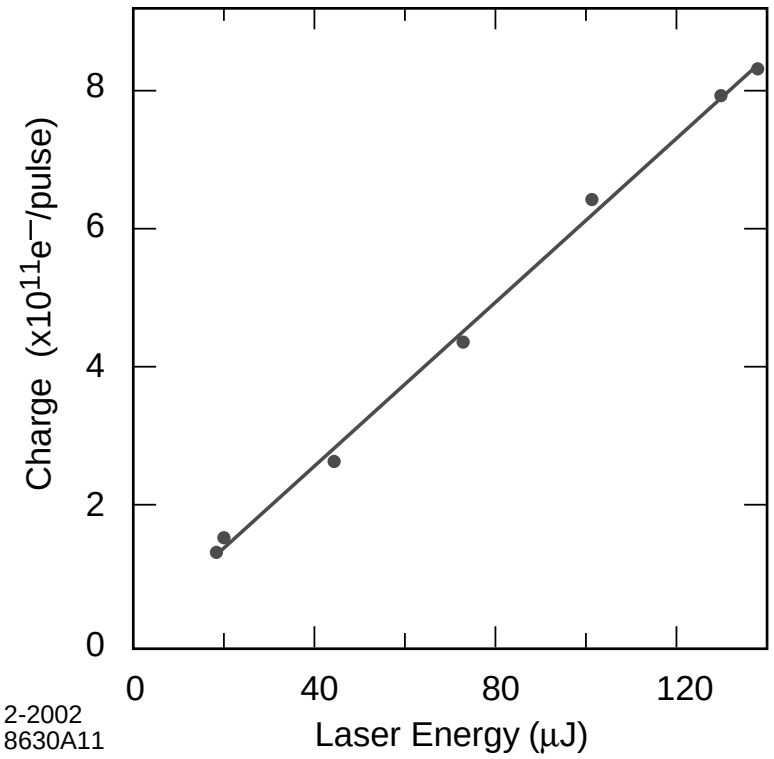
Charge (x10^11 e^−/pulse)
0
2
4
6
8
0
40
80
120
Laser Energy (µJ)
2-2002
8630A11

FIGURE 11

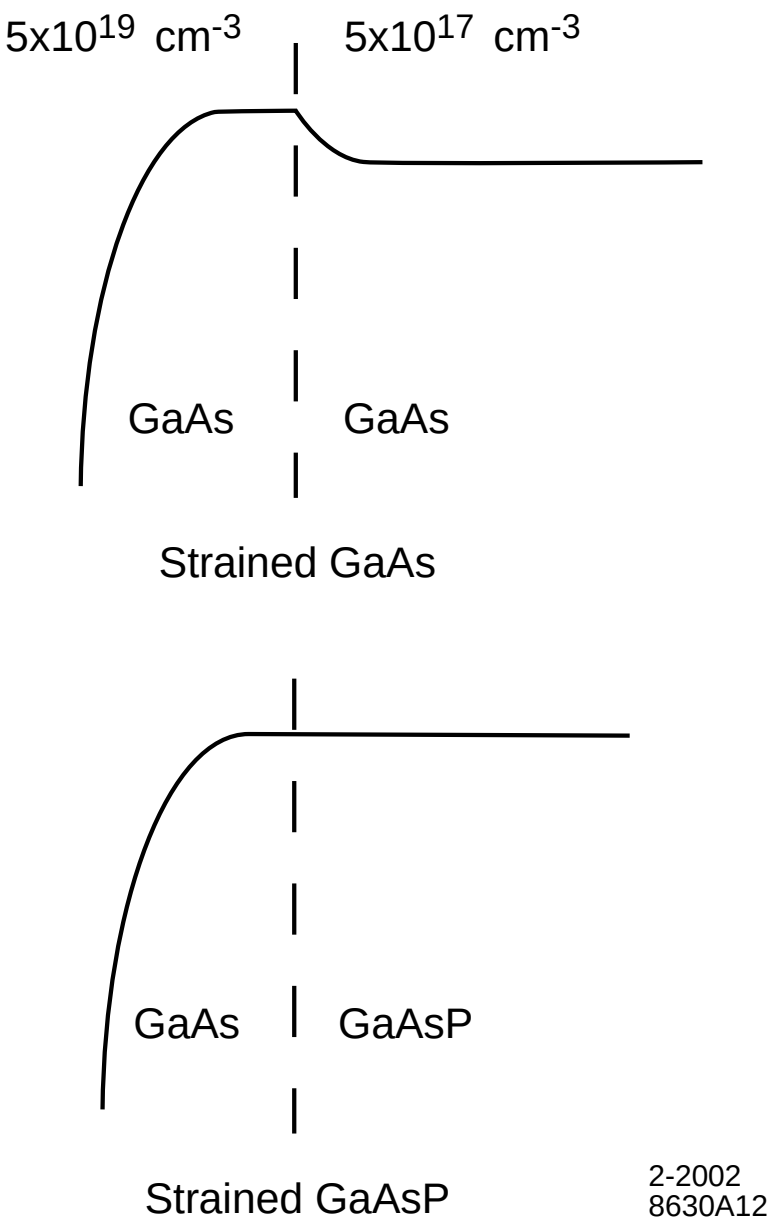
5x10^19 cm^-3
5x10^17 cm^-3
GaAs
GaAs
Strained GaAs
GaAs
GaAsP
Strained GaAsP
2-2002
8630A12

FIGURE 12

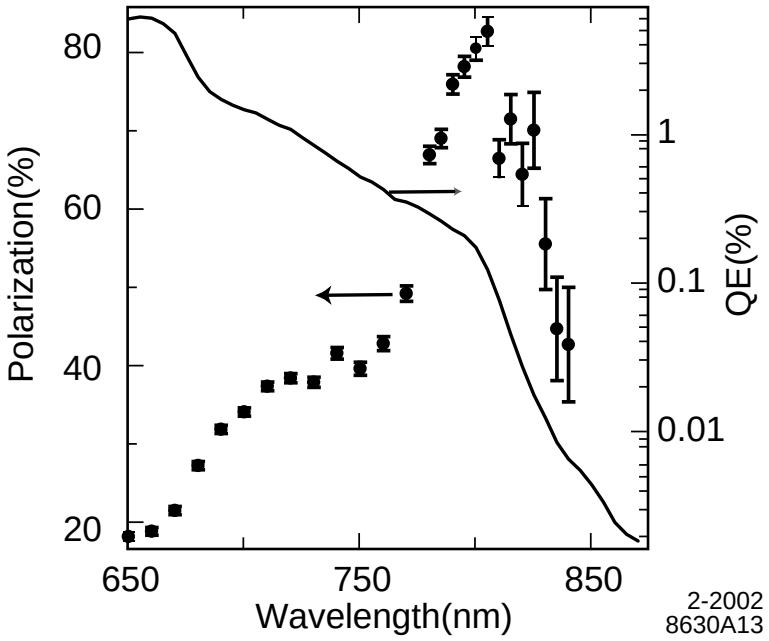
80
60
40
20
Polarization(%)
650
750
850
Wavelength(nm)
1
0.1
0.01
QE(%)
2-2002
8630A13

FIGURE 13

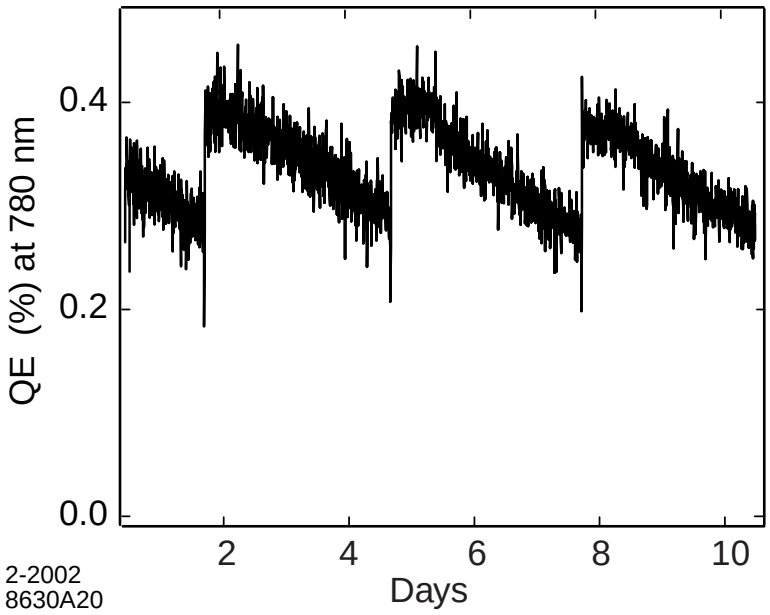

FIGURE 14

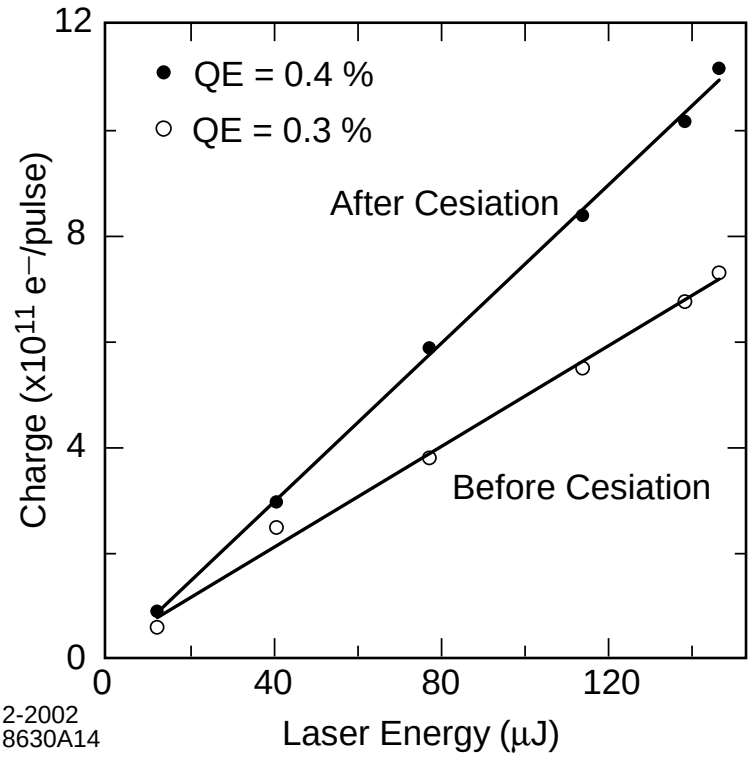
12
8
4
0
0
40
80
120
QE = 0.4 %
QE = 0.3 %
After Cesiation
Before Cesiation
Charge (x10^11 e^−/pulse)
Laser Energy (μJ)
2-2002
8630A14

FIGURE 15

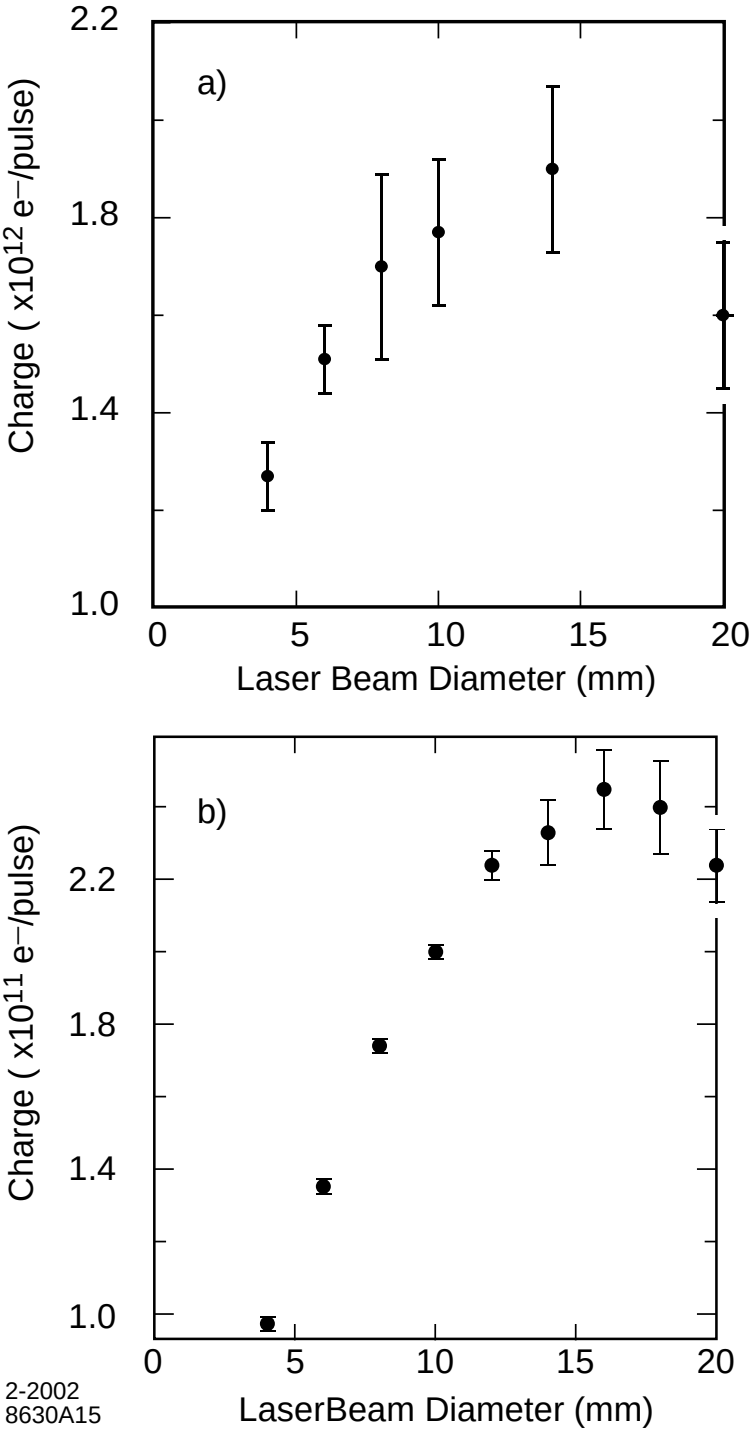
a)
Charge (x10^12 e−/pulse)
2.2
1.8
1.4
1.0
0
5
10
15
20
Laser Beam Diameter (mm)
b)
Charge (x10^11 e−/pulse)
2.2
1.8
1.4
1.0
0
5
10
15
20
LaserBeam Diameter (mm)
2-2002
8630A15

FIGURE 16

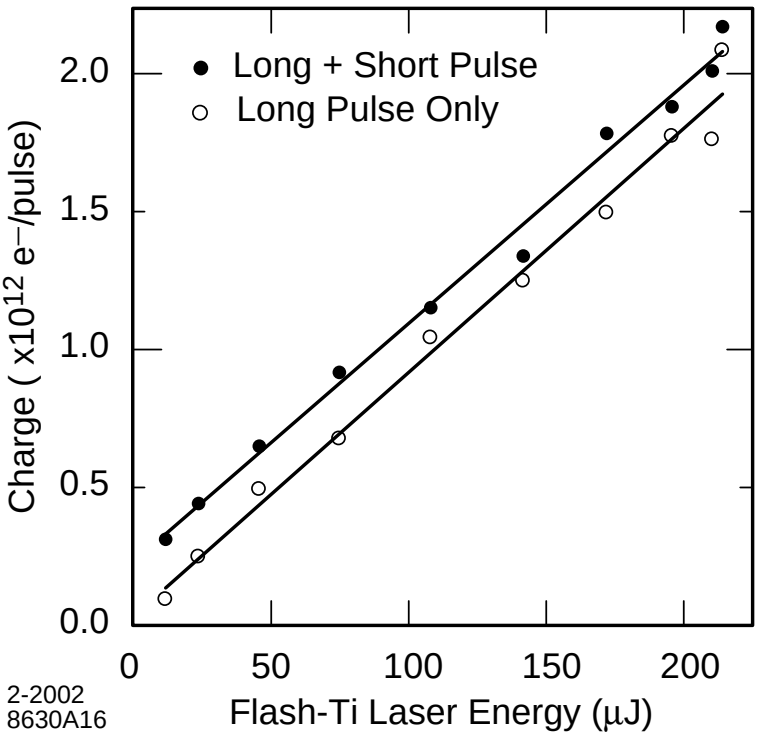
Long + Short Pulse
Long Pulse Only
Charge (x10^12 e−/pulse)
2.0
1.5
1.0
0.5
0.0
0
50
100
150
200
Flash-Ti Laser Energy (μJ)
2-2002
8630A16

FIGURE 17

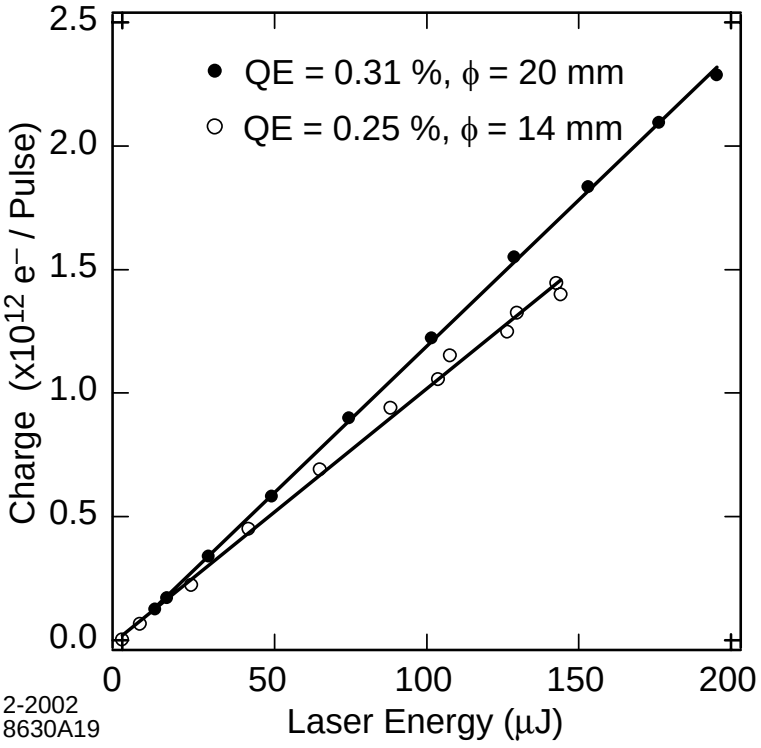
QE = 0.31 %, ϕ = 20 mm
QE = 0.25 %, ϕ = 14 mm
Charge (x10^12 e⁻ / Pulse)
Laser Energy (µJ)
0.0
0.5
1.0
1.5
2.0
2.5
0
50
100
150
200
2-2002
8630A19

FIGURE 18